

粉煤灰漂珠负载 Bi_2WO_6 复合材料的制备及光催化性能研究

张 进^{*,1} 崔 皓² 翟建平²

(¹ 南京晓庄学院生物化工与环境工程学院, 南京 211171)

(² 污染控制与资源化研究国家重点实验室, 南京大学环境学院, 南京 210046)

摘要: 以工业固体废弃物粉煤灰漂珠(fly ash cenospheres, FACs)为载体, 采用水热法制备了新颖的漂珠负载 Bi_2WO_6 复合材料($\text{Bi}_2\text{WO}_6/\text{FACs}$), 通过 X 射线衍射(XRD), 扫描电子显微镜(SEM), X-射线光电子能谱(XPS), 和紫外-可见漫反射光谱(DRS)技术对其进行了表征。XRD 数据展示了正交相 Bi_2WO_6 的特征衍射峰。DRS 结果证实了引入 FACs 后 Bi_2WO_6 对可见光的吸收增强。在可见光的照射下, 以亚甲基蓝溶液的光催化降解评价了 $\text{Bi}_2\text{WO}_6/\text{FACs}$ 复合材料的光催化性能。结果表明: $\text{Bi}_2\text{WO}_6/\text{FACs}$ 的光催化性能优于纯 Bi_2WO_6 的, 其一级反应速率常数(k)为后者的 2.4 倍。尤其是由于漂珠质轻中空的特性, $\text{Bi}_2\text{WO}_6/\text{FACs}$ 复合光催化剂可长时间漂浮于水面, 既能充分吸收光能, 又有利于催化剂的回收和重复利用。

关键词: 复合材料; Bi_2WO_6 ; 粉煤灰漂珠; 可见光

中图分类号: O614.53²; O614.61³

文献标识码: A

文章编号: 1001-4861(2014)12-2857-06

DOI: 10.11862/CJIC.2014.395

Synthesis of Bi_2WO_6 /Fly Ash Cenospheres Composites with Enhanced Photocatalytic Properties

ZHANG Jin^{*,1} CUI Hao² ZHAI Jian-Ping²

(¹School of Biochemical and Environmental Engineering, Nanjing Xiaozhuang University, Nanjing 211171, China)

(²State Key Laboratory of Pollution Control and Resource Reuse,
and School of the Environment, Nanjing University, Nanjing 210023, China)

Abstract: A fly ash cenospheres supported Bi_2WO_6 composites ($\text{Bi}_2\text{WO}_6/\text{FACs}$) photocatalysts were prepared by a hydrothermal method. The composites were characterized by X-ray diffraction (XRD), scanning electron microscope (SEM), X-ray photoelectron spectra (XPS), and UV-Vis diffused reflectance spectroscopy (DRS) techniques. The XRD patterns exhibited characteristic diffraction peaks of orthorhombic phase of Bi_2WO_6 . The DRS results showed that the visible light absorption of the $\text{Bi}_2\text{WO}_6/\text{FACs}$ composite is enhanced. The as-prepared material exhibited good photocatalytic activity for the degradation of methylene blue (MB) under visible light irradiation, and the first-order reaction rate constant (k) of 0.012 min^{-1} for $\text{Bi}_2\text{WO}_6/\text{FACs}$ composite is higher than 0.0048 min^{-1} of pure Bi_2WO_6 . Moreover, the present study provides a useful strategy to design heterogeneous catalysis, in which catalytic materials are supported on fly ash cenospheres, an industrial solid waste produced from coal-firing power plants.

Key words: composites; Bi_2WO_6 ; fly ash cenospheres (FACs); visible-light

收稿日期: 2014-07-04。收修改稿日期: 2014-09-12。

国家自然科学基金(No.51308282), 中国博士后科学基金(No.2012M511254)和江苏省高校自然科学基金项目(No.12KJD610004)资助项目。

*通讯联系人。E-mail: jzmary@163.com, Tel: 13805154407

0 Introduction

Environmental pollution is a serious problem in the world. The amount of organic pollutants in wastewater streams and volatile organic compounds in the atmosphere has continuously increased over the last few decades. New approaches are urgently needed to solve this problem. Photocatalytic oxidation using semiconductors is a promising technology to reduce and eliminate these contaminants from the environment^[1]. It has been demonstrated that many organic pollutants present in water or air stream can be removed by means of photocatalytic oxidation^[2-4]. Therefore, the environmentally sound materials that can photocatalytically oxidize and degrade harmful organic compounds have attracted considerable interest. Among the photocatalytic materials, the multicomponent metal oxides containing bismuth were regarded as the excellent visible-light-driven photocatalysts. Very recently, Bi_2WO_6 , with a band gap of 2.6~2.8 eV, has attracted increasing attentions due to its good photocatalytic performance in the degradation of organic pollutants and water splitting under visible light irradiation. Besides, Bi_2WO_6 has exhibited excellent intrinsic physical and chemical properties, such as ferroelectric piezoelectricity, catalytic activity, non-linear dielectric susceptibility, and luminescent properties^[5-9].

However, there are some drawbacks to using the Bi_2WO_6 in powder form during photocatalytic processes: the suspended powder tends to aggregate, and is difficult to separate from the water after the reaction. Therefore, the load of Bi_2WO_6 powders on the microsphere cores could allow them not only to retain high activity but also enable easy recollection of the catalysts after reaction^[10].

Coal fly ash (CFA) is generated during the combustion of pulverized coal in coal-fired power stations. With the development of power industry, fly ash emissions from coal-fired power plants have increased year by year. As such it is an industrial by-product that if not put to beneficial use, is a recognized environmental pollutant^[11]. The lightweight

fraction of CFA is widely known as cenospheres, which means hollow sphere. The fact that the fly ash cenospheres (FACs) float on water make them used as a buoyant carrier to enhance catalytic activity as they increase the exposure of the particle to light sources^[12-13]. And they float also means that they are easily recovered from water after the reaction. This feature of the cenospheres has also attracted interest for their use in water purification applications^[14-15].

Herein, fly ash cenospheres (FACs) were employed as a support for the highly active Bi_2WO_6 structure, and a new $\text{Bi}_2\text{WO}_6/\text{FACs}$ heterogeneous photocatalyst was prepared via a hydrothermal method. The prepared samples showed high visible light photocatalytic activity for the photocatalytic degradation of methylene blue (MB) aqueous solution.

1 Experimental

1.1 Materials

All the reagents were of analytical grade and were used as received from Sinopharm (China). The FACs were obtained from Nanjing Jinling Petrochemical Company. First, the FACs were sieved and the particles with the size range of 100~125 μm were chosen as following experimental material. Then, the sieved FACs were treated ultrasonically in 10% dilute nitric acid for 1 h. Finally, these particles were filtered and washed with deionized water, followed by drying in a vacuum drying oven at 120 $^\circ\text{C}$ for 3 h.

1.2 Preparation of $\text{Bi}_2\text{WO}_6/\text{FACs}$ composites

In a typical process, $\text{Bi}(\text{NO}_3)_3 \cdot 5\text{H}_2\text{O}$ (2.43 g) was dissolved in 40 mL of deionized water, to which 2 mL 65% HNO_3 was added under vigorous stirring. Meanwhile, $\text{Na}_2\text{WO}_4 \cdot 2\text{H}_2\text{O}$ (0.82 g) and 0.5 g of SDS were dissolved in 40 mL of deionized water. After that, these two solutions were mixed together and the pH value of this mixed solution was adjusted to 9 using given amounts of NaOH solution. After sonication for 30 min, the white precipitate was collected by centrifugation, washed with deionized water, and dried at 100 $^\circ\text{C}$ for 5 h. The amorphous Bi_2WO_6 precursor was acted as one of starting materials. Then, $\text{Bi}_2\text{WO}_6/\text{FACs}$ composites were synthesized via a hydrothermal

method. Briefly, 1 g of amorphous Bi_2WO_6 was dispersed into 30 mL deionized water by ultrasonic treatment. Subsequently, 3 g of FACs were added into the solution and sonicated for 1 h to get the mixed precursor suspension. The suspension was then transferred into a 50 mL Teflon autoclave and maintained at 180 °C for 24 h. The final products were washed with distilled water for several times, and finally dried at 80 °C for 6 h. For comparison, pure Bi_2WO_6 was also prepared in the same way.

1.3 Characterization

Powder X-ray diffraction (XRD) patterns were obtained on an X' TRA diffract meter (ARL, Switzerland) using $\text{Cu K}\alpha$ radiation to determine the crystal phase of the synthesized samples. Scanning electron microscopic (SEM) analysis was performed using an S-3400NII (Hitachi, Japan) scanning electron spectroscope, equipped with an EX-250 (Horiba, Japan) microscope probe for the energy dispersive X-ray analysis (EDX). X-ray photoelectron spectra (XPS) were measured on an ESCALAB 250 spectrometer (Thermo Fisher Scientific, Waltham, MA) with an $\text{Al K}\alpha$ X-ray source (1 486.6 eV). The binding energies of all peaks were checked against the C1s line (284.6 eV) originating from surface impurity carbons. UV-Vis diffuse reflectance spectra were recorded on a UV-2450 spectroscopy (Shimadzu, Japan) with barium sulfate as the reference sample. The reflectance spectra of the catalysts were analyzed under ambient conditions in the wavelength range of 380~800 nm.

1.4 Photocatalytic degradation of MB

The as-prepared photocatalysts were evaluated for photocatalytic degradation of MB dye solution. The optical system consists of a 500 W xenon (Xe) lamp and a UV cut-off filter to remove any radiation below 420 nm. The Xe lamp was surrounded by a quartz jacket and placed within the inner part of a quartz reactor vessel (Nanjing JYZCPST Co., Ltd.), through which a suspension of MB and the photocatalyst was circulated. An outer recycling water glass jacket maintained a constant reaction temperature (25 °C). In a typical photocatalytic activity test, 0.2 g as-prepared catalyst was added into a 50 mL MB solution (10 $\text{mg}\cdot\text{L}^{-1}$), then the dispersion was kept in dark for 60 min to obtain the adsorption equilibrium state. During the irradiation, the temperature of the solution was maintained by cooling water. Aliquots were withdrawn from the irradiated solutions at appropriate intervals and analyzed by UV-Vis spectroscopy (Shimadzu, UV-2550) at 664 nm for MB.

Photolysis experiments were performed, without photocatalyst, using the same experimental setup previously described for the photocatalytic system.

2 Results and discussion

2.1 XRD analysis

XRD patterns of the FACs, Bi_2WO_6 , and the $\text{Bi}_2\text{WO}_6/\text{FACs}$ samples are shown in Fig.1. The XRD pattern of Fig.1 (c) indicates that all the peaks coincide with the orthorhombic phase of Bi_2WO_6 according to the JCPDS card No. 39-0256. Moreover, the XRD patterns of $\text{Bi}_2\text{WO}_6/\text{FACs}$ composite in Fig.1 (b) demonstrate the presence of orthorhombic Bi_2WO_6 . But the diffraction intensity of Bi_2WO_6 becomes weak, implying that the crystallinity of Bi_2WO_6 is weakened by the introduction of FACs.

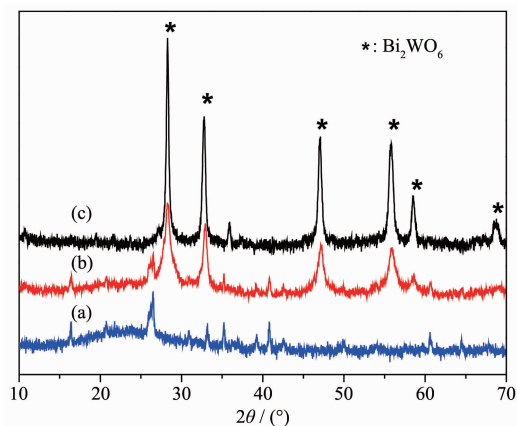


Fig.1 XRD patterns of (a) FACs, (b) $\text{Bi}_2\text{WO}_6/\text{FACs}$, and (c) Bi_2WO_6 samples

2.2 SEM and EDX analysis

SEM micrographs of the FACs and $\text{Bi}_2\text{WO}_6/\text{FACs}$ samples are shown in Fig.2. The pristine FACs in Fig. 2a~b exhibited a relatively uniform smooth surface with a diameter of 100~120 μm . As shown in Fig.2c, the FAC has hollow structure. The SEM picture (Fig. 2d~e) of $\text{Bi}_2\text{WO}_6/\text{FACs}$ shows that this catalyst contains

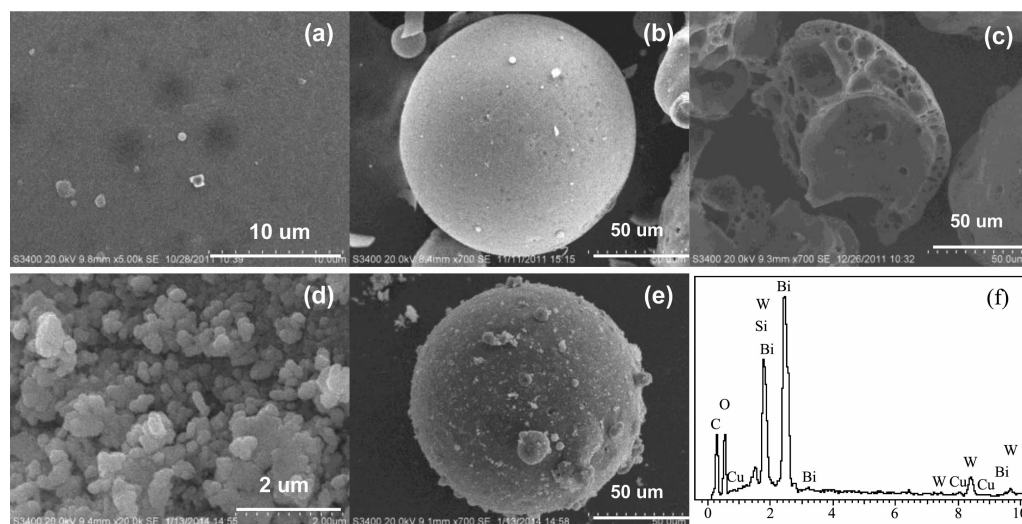


Fig.2 SEM images of the catalysts (a~c) FACS; (d~e) $\text{Bi}_2\text{WO}_6/\text{FACS}$; and (f) EDX spectra of the $\text{Bi}_2\text{WO}_6/\text{FACS}$ composite

irregular shaped particles which are the aggregates of tiny crystals and the distribution on surface of FACS is not uniform. The chemical compositions of $\text{Bi}_2\text{WO}_6/\text{FACS}$ composites were determined using EDX technique attached on the SEM. As shown in Fig.2f, the EDX spectra of the composites show strong signals from Bi, W, and O elements, confirming the presence of Bi, W, and O elements in the composites. Thus, the combined results of XRD, SEM and EDX suggest that the Bi_2WO_6 particles were loaded successfully on the surface of FACS.

2.3 XPS analysis

The XPS spectra of the FACS and $\text{Bi}_2\text{WO}_6/\text{FACS}$ samples are presented in Fig.3. As shown in Fig.3a, the surfaces of the pristine FACS particles were composed mainly of C, Si, Al and O elements. Obviously, Bi and W elements orbitals can be identified in the XPS spectra of the $\text{Bi}_2\text{WO}_6/\text{FACS}$ composite (Fig.3b). Two peaks with binding energies

around 464.5 and 440.9 eV can be clearly seen in Fig.3b, which can be ascribed to the signals of $\text{Bi}4d_{5/2}$ and $\text{Bi}4d_{3/2}$.

Fig.3c~d show $\text{W}4f$ and $\text{Bi}4f$ high-resolution XPS spectra of the as-fabricated $\text{Bi}_2\text{WO}_6/\text{FACS}$ samples. The peaks at 37.5 and 35.3 eV in $\text{Bi}_2\text{WO}_6/\text{FACS}$ samples correspond to $\text{W}4f_{5/2}$ and $\text{W}4f_{7/2}$, respectively, both of which can be assigned to the W^{6+} oxidation state^[17]. In Fig.3d, it is obvious that $\text{Bi}4f$ consists of two peaks with binding energies around 158.0 and 163.4 eV, corresponding to the signals from doublets of $\text{Bi}4f_{7/2}$ and $\text{Bi}4f_{5/2}$ in the trivalent oxidation state.

2.4 DRS analysis

The UV-Vis diffuse reflection spectra (DRS) of the as-prepared samples were shown in Fig.4. According to the spectra, the absorption edge of pure Bi_2WO_6 and $\text{Bi}_2\text{WO}_6/\text{FACS}$ composite were around 450 nm and 470 nm, respectively. Compared with the pure Bi_2WO_6 , the light absorption ability of $\text{Bi}_2\text{WO}_6/\text{FACS}$

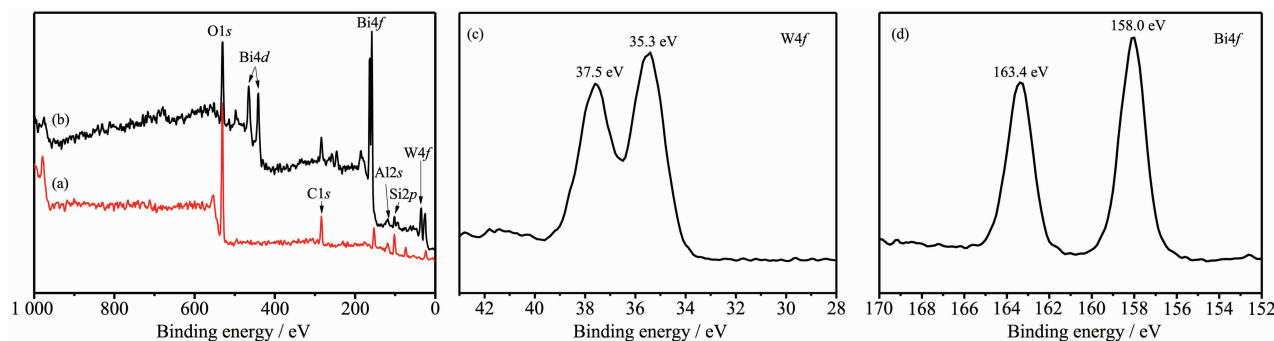


Fig.3 XPS spectra of (a) FACS, (b) $\text{Bi}_2\text{WO}_6/\text{FACS}$; and high-resolution XPS spectra of $\text{Bi}_2\text{WO}_6/\text{FACS}$: (c) $\text{W}4f$, (d) $\text{Bi}4f$

composite is enhanced within the visible light range 450~800 nm (Fig.4a). For a crystalline semiconductor, the band gap energy of a semiconductor can be calculated by the equation (1):

$$\alpha h\nu = A(h\nu - E_g)^{n/2} \quad (1)$$

where α , ν , E_g , and A are absorption coefficient, light frequency, band gap, and a constant, respectively. Among them, n is determined from the type of optical transition of a semiconductor, and the value of n for the direct semiconductor (such as Bi_2WO_6) is 1. The band-gap energy of samples can be thus estimated from a plot of $(\alpha h\nu)^2$ vs photon energy ($h\nu$). The intercept of the tangent to the x -axis will allow a good approximation of the band-gap energy for a semiconductor^[6,18]. Therefore, the band gaps of Bi_2WO_6 and $\text{Bi}_2\text{WO}_6/\text{FACs}$ were determined to be 2.85 and 2.72 eV, respectively (Fig.4b). It is relatively lower than that of commercial photocatalyst $\text{TiO}_2\text{-P25}$ (3.2 eV), indicating that the as-prepared $\text{Bi}_2\text{WO}_6/\text{FACs}$ composite is more suitable for photocatalytic

application under visible-light irradiation^[19].

2.5 Photocatalytic activity

The photocatalytic activity of the as-prepared photocatalysts was studied under visible light irradiation and MB was selected as the model pollutant. Fig.5(a) shows the photocatalytic degradation efficiency of MB by different photocatalysts. The direct photolysis of MB was only 6% after 210 min irradiation, indicating that MB self-degradation was almost negligible. The photodegradation rates of MB reached 92% after irradiation for 210 min in the presence of the $\text{Bi}_2\text{WO}_6/\text{FACs}$ samples, while the photodegradation rate of MB over pure Bi_2WO_6 was 64% after irradiation for 210 min under the same conditions.

Moreover, to quantitatively study the reaction kinetics of the MB degradation, the experimental data were fitted by the Langmuir-Hinshelwood model, and the model was expressed by the equation (2):

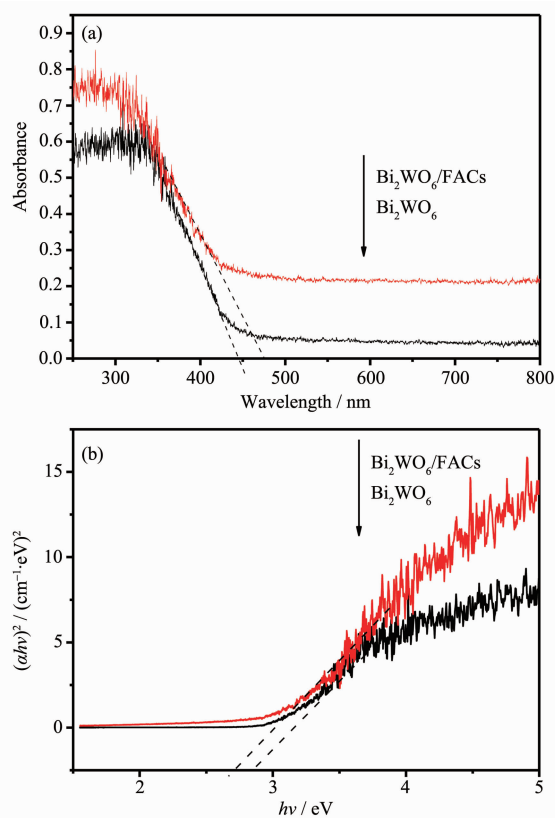


Fig.4 (a) UV-Vis diffuse reflectance spectra of samples; (b) band gap evaluation for linear dependence of $(\alpha h\nu)^2$ versus photon energy ($h\nu$) for the samples

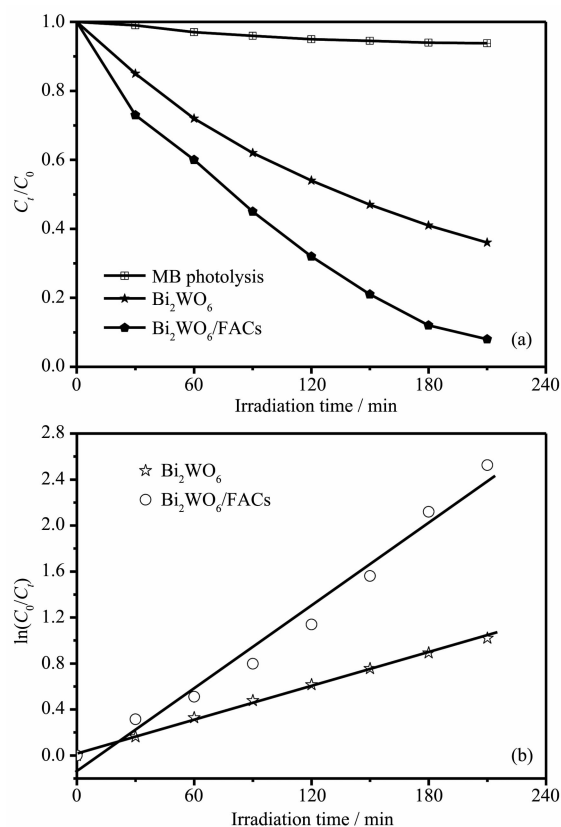


Fig.5 (a) Degradation rates of MB under visible light irradiation with different samples; (b) First-order kinetics data for the photodegradation of MB over different samples

$$k = \frac{1}{t} \ln \frac{C_0}{C_t} \quad (2)$$

where k is the apparent first-order reaction rate constant (min^{-1}), C_0 is the initial MB concentration and C_t is the MB concentration at reaction time of t (min). As shown in Fig.5b, all fitting curves of the irradiation time (t) against $\ln(C_0/C_t)$ are nearly linear. The k was calculated to be 0.004 8 and 0.011 9 min^{-1} corresponding to pure Bi_2WO_6 and $\text{Bi}_2\text{WO}_6/\text{FACs}$, respectively. Obviously, the rate constant for $\text{Bi}_2\text{WO}_6/\text{FACs}$ sample is approximately 2.4 times higher than that pure Bi_2WO_6 . The improved photocatalytic activity of the $\text{Bi}_2\text{WO}_6/\text{FACs}$ composite may be attributable to: (1) presence of FACs can absorb more MB on the surface of this substrate, and increasing the rate of photocatalytic process^[20]; (2) the FACs acted as a dispersing support to inhibit grain growth, which contributed to making full use of light for photocatalysis^[21]; (3) the absorption band of the $\text{Bi}_2\text{WO}_6/\text{FACs}$ is red-shift compared with the pure Bi_2WO_6 , which could favor light absorption and facilitate photocatalytic reaction^[22-23].

3 Conclusions

In this paper, $\text{Bi}_2\text{WO}_6/\text{FACs}$ composites were prepared by a hydrothermal method. The composites exhibit much enhanced activity in degradation of MB in comparison with pure Bi_2WO_6 under visible light irradiation. The first-order reaction rate constant for $\text{Bi}_2\text{WO}_6/\text{FACs}$ sample is approximately 2.4 times higher than that pure Bi_2WO_6 . Additionally, the present study provides a useful strategy to design heterogeneous catalysis, in which catalytic materials are supported on FACs. The FACs, industrial by-product generated in coal-firing power plants, are used as support with low cost and nontoxicity. The $\text{Bi}_2\text{WO}_6/\text{FACs}$ could float on the water owing to low density, the $\text{Bi}_2\text{WO}_6/\text{FACs}$ thus can be easily recovered by filtration.

References:

- [1] Zhou Y, King D M, Liang X H, et al. *Appl. Catal. B: Environ.*, **2010**,**10**:54-60
- [2] Lin F, Zhang Y N, Wang L, et al. *Appl. Catal. B: Environ.*, **2012**,**127**:363-370
- [3] Asahi R, Morikawa T, Ohwaki T, et al. *Science*, **2001**,**293**:269-273
- [4] Pirakanniemi K, Sillanpaa M. *Chemosphere*, **2002**,**48**:1047-1060
- [5] Zhang J, Zheng H H, Xu Y, et al. *J. Am. Chem. Soc.*, **2013**, **96**(5):1562-1569
- [6] Ju P, Wang P, Li B, et al. *Chem. Eng. J.*, **2014**,**236**:430-437
- [7] Zhang L S, Wang H L, Chen Z G, et al. *Appl. Catal. B: Environ.*, **2011**,**106**:1-13
- [8] Sheng J Y, Li X J, Xu Y M. *ACS Catal.*, **2014**,**4**:732-737
- [9] CUI Yu-Min (崔玉民), HONG Wen-Shan (洪文珊), LI Hui-Quan (李慧泉), et al. *Chinese J. Inorg. Chem.* (无机化学学报), **2014**,**30**(2):431-441
- [10] Zhang Z J, Wang W Z, Jiang D, et al. *Appl. Surf. Sci.*, **2014**,**292**:948-953
- [11] Blissett R S, Rowson N A. *Fuel*, **2012**,**97**:1-23
- [12] Wang B, Li Q, Wang W, et al. *Appl. Surf. Sci.*, **2011**,**257**:3473-3479
- [13] Zhang J, Cui H, Wang B, et al. *Chem. Eng. J.*, **2013**,**223**:737-746
- [14] Huo P, Yan Y, Li S, et al. *Desalination*, **2010**,**263**:258-263
- [15] Xu X T, Li Q, Cui H, et al. *Desalination*, **2011**,**272**:233-239
- [16] Sun Z H, Guo J J, Zhu S M, et al. *Nanoscale*, **2014**,**6**:2186-2193
- [17] LI Hai-Xia (李海霞), TANG Wu (唐武), WENG Xiao-Long (翁小龙), et al. *Chinese Rare Met. Mater. Eng.* (稀有金属材料与工程), **2008**,**37**(7):1213-1216
- [18] Tian Y L, Chang B B, Yang Z C, et al. *RSC Adv.*, **2014**,**4**:4187-4193
- [19] Feng T, Wang X D, Feng G S. *Mater. Lett.*, **2013**,**100**:36-39
- [20] Jafry H R, Liga M V, Li Q, et al. *New J. Chem.*, **2011**,**35**:400-406
- [21] Sakthivel S, Shankar M V, Palanichamy M, et al. *Water Res.*, **2004**,**38**:3001-3008
- [22] Zhai C Y, Zhu M S, Ren F F, et al. *J. Hazard. Mater.*, **2013**, **263**:291-298
- [23] Zhai C Y, Zhu M S, Lu Y T, et al. *Phys. Chem. Chem. Phys.*, **2014**,**16**:14800-14867